

# Synthesis, crystalline inclusion and structural study of bulkily stoppered and rigid framework molecular constructions

Torsten Müller, Wilhelm Seichter and Edwin Weber\*

Received (in Durham, UK) 15th November 2005, Accepted 23rd February 2006

First published as an Advance Article on the web 20th March 2006

DOI: 10.1039/b516244k

A series of compounds **1–5** featuring a structure composed of linear or trigonal ethynyl and aryl containing rigid construction elements with attached terminal adamantyl stoppers were synthesized to study their structures and enclathrating properties. While only the linear tetraethynylene prototype molecule **1** exhibited versatile inclusion behavior, the compounds **2–5** were found to be inefficient. X-Ray crystal structures of the inclusion compounds between **1** and THF, cyclohexanol and aniline as well as of the unsolvated compounds **3**, **4** and **5** are reported, throwing light on the respective modes of crystalline packing affected by molecular dimension and shape parameters.

## Introduction

Shape persistent framework molecules<sup>1</sup> and other rigid molecular constructions<sup>2</sup> are of high current interest due to their potential use in the formation of molecular containers<sup>3</sup> and sorptive porous materials.<sup>4</sup> They are also an essential part of spacer type supramolecular devices.<sup>5</sup> Moreover, molecules providing rigid and bulky constitutions have attracted considerable attention regarding their ability to yield inclusion compounds<sup>6,7</sup> and engineered functional architectures<sup>8,9</sup> in the crystalline state. Molecular shape, geometry and dimensions are considered important parameters in this respect.<sup>10</sup>

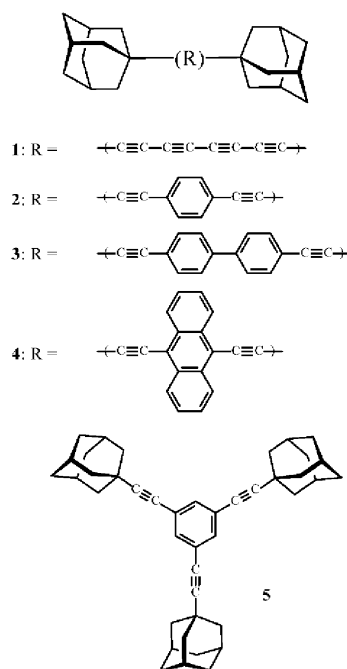
In a previous study,<sup>11</sup> we have shown that certain types of dumb-bell shaped molecules featuring an oligoalkyne linear spacer unit with bulky terminal adamantyl substituents, of which compound **1** is a typical example, are prone to forming an open channel structure when cocrystallized with suitable solvent molecules. Desolvation experiments provided evidence for the reversible inclusion of guests and partial substitution by asymmetrical long-chain chromophores during recrystallization was shown to yield compounds with non-linear optical properties.

This has stimulated an examination of the structurally related compounds **2–5** (Scheme 1) which are of the same kind with reference to the bulky adamantyl stoppers but differ in the nature of the central spacer unit, with alkynes being partly replaced by aromatic groups, that gives rise to linear (**2–4**) and trigonal (**5**) modifications of the parent compound (**1**). Synthesis of **2–5**, inclusion behavior of **1** and crystal structures of respective compounds are reported, involving inclusion complexes of chemical composition: **1** with THF (1 : 1), cyclohexanol (2 : 7) and aniline (3 : 5) as well as the unsolvated compounds **3–5**.

## Results and discussion

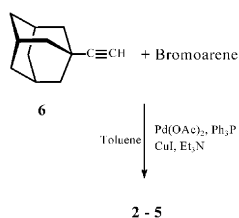
### Synthesis and crystalline inclusion formation

Differing from the synthesis of **1**,<sup>11</sup> the new compounds **2–4** (Scheme 1) were prepared from 1-ethynyladamantane (**6**) and the corresponding aryl bromides (1,4-dibromobenzene, 4,4'-dibromobiphenyl, 9,10-dibromoanthracene and 1,3,5-tribromobenzene, respectively) by using the conditions of a palladium catalyzed coupling reaction,<sup>12</sup> which was carried out under argon in boiling toluene in the presence of diethylamine with a mixture of catalyst, composed of triphenylphosphane, Pd(II) acetate and Cu(I) iodide (Scheme 2). The 1-ethynyladamantane (**6**) was synthesized from 1-bromoadamantane and vinyl bromide in the presence of aluminium bromide as



Scheme 1 Chemical structures of compounds.

Institute of Organic Chemistry, TU Bergakademie Freiberg, Leipziger Straße 29, 09596 Freiberg/Sachs., Germany. E-mail: edwin.weber@chemie.tu-freiberg.de; Fax: +49 (0) 37 31/39-31 70



Scheme 2 Synthesis of compounds.

catalyst, followed by double dehydrobromination with potassium hydroxide in dimethyl sulfoxide, according to literature procedures.<sup>13,14</sup>

Crystallization of **1** from solvents such as those specified in Table 1 yielded the respective solvent inclusion compounds that are detailed with stoichiometric data in the table. As shown in the listing, inclusion complexes of **1** are formed with solvents of different classes of compounds, but mostly involving solvents of an aprotic (except cyclohexanol and aniline), lower polar or apolar nature, which is in line with the polarity behavior of **1**. Nevertheless, a number of other potential solvents, specified in Table 1, which were also tested, did not yield respective inclusion compounds, suggesting selectivity of inclusion formation. This refers not only to the property of polarity but also to the shape and size parameters of the solvent molecules. Thus, the linear hydrocarbons from pentane to heptane are included, but octane, decane and cyclohexane, which are of greater length or diameter, failed. In a similar way, this is also the case for toluene, which is included, while the higher substituted xylenes and mesitylene failed.

The most surprising finding, however, is that none of the modified compound structures, such as those provided by **2–5**, yielded an inclusion compound under the same recrystallization conditions with any of the solvents given in Table 1. On the contrary, in each of these cases the unsolvated compounds **2–5** were isolated. This suggests a markedly different packing behavior of the molecules **2–5** compared to **1** in the crystals, inviting a structural study.

Table 1 Crystalline inclusion compounds of **1**

Guest solvent <sup>a</sup>	Host : guest stoichiometric ratio <sup>b</sup>
<i>n</i> -Pentane	1 : 2
<i>n</i> -Hexane	2 : 3
<i>n</i> -Heptane	2 : 5
Toluene	1 : 3
Chloroform	1 : 1
1,2-Dichloroethane	1 : 1
2-Bromobutane	1 : 1
Acetone	3 : 2
2-Butanone	1 : 1
2-Pentanone	1 : 2
Ethyl acetate	1 : 2
Tetrahydrofuran	1 : 1
Cyclohexanol	2 : 7
Aniline	3 : 5

<sup>a</sup> Octane, decane, cyclohexane, xylenes, mesitylene, dichloromethane, tetrachloroethene, cyclohexanone, acetonitrile, *N,N*-dimethylformamide, 1,4-dioxane, methanol, ethanol, 1-propanol, 2-propanol, 1-butanol, benzyl alcohol, which were also tested as guest solvents, yielded no inclusion compounds. <sup>b</sup> Host : guest chemical composition ratios were determined by <sup>1</sup>H NMR integration.

## Inclusion compounds of **1**

Detailed crystal structures of inclusion compounds of **1** with chemical compositions **1**·2-butanone (1 : 1) and **1**·2-bromobutane (1 : 1), both featuring a channel-type packing, have previously been described.<sup>11</sup> In order to show the structural broadness of the inclusion compounds of **1** formed, three additional inclusion compounds that clearly differ either in the stoichiometric ratio or in the nature of the solvent, *i.e.* **1**·THF (1 : 1), **1**·cyclohexanol (2 : 7) and **1**·aniline (3 : 5) (Table 1), were selected for X-ray structure determination.

The crystal structure of the inclusion compound of **1** with tetrahydrofuran (**1a**) crystallizes in the monoclinic space group *P*2<sub>1</sub>/*c*, with two crystallographically independent host molecules and one and two halves of guest molecules in the asymmetric unit of the cell (Fig. 1). Consequently, the host molecules are asymmetric and two of the guest molecules are disordered around symmetry centers ( $\frac{1}{2}$ ,  $\frac{1}{2}$ ,  $\frac{1}{2}$  and 0,  $\frac{1}{2}$ , 0). The host molecules have a length of approximately 19.6 Å and show a slight S-shaped deformation along the tetraethynylene spacer, probably due to packing effects. Within experimental error, the bond distances within the C<sub>8</sub>-fragment are identical for both molecules. They are C(1)–C(11) 1.470(3), C(11)–C(12) 1.199(4), C(12)–C(13) 1.370(4), C(13)–C(14) 1.213(4), C(14)–C(15) 1.352(4), C(15)–C(16) 1.217(4), C(16)–C(17) 1.364(4), C(17)–C(18) 1.198(4), C(18)–C(19) 1.467(3) Å indicating partial polyene bonding.

The packing in the crystal is characterized by a channel structure (Fig. 2), resembling that of the corresponding inclusion compound with 2-butanone.<sup>11</sup> The channels, being occupied by the guest molecules of THF, are formed by the host molecules and have a minimum cross-section of nearly 8.2 × 5.6 Å. The inner surface of the channels consists of adamantyl and ethynylene chain fragments facing each other.

Crystallization of **1** from cyclohexanol yields an inclusion compound (**1b**) of space group *P*1̄, with one independent host molecule and three and one half guest molecules in the asymmetric unit of the cell, *i.e.* also here the molecular

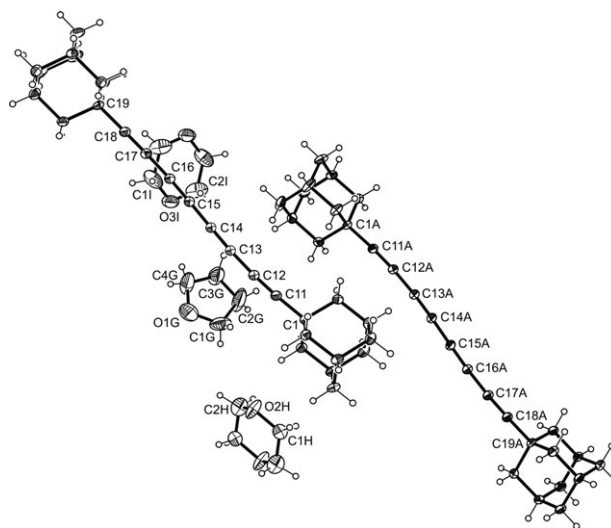
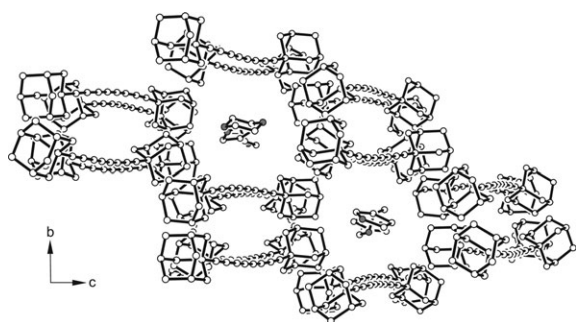


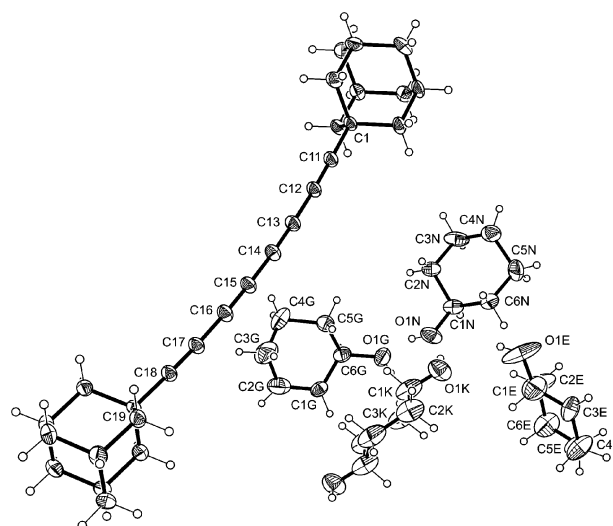
Fig. 1 Molecular structure of the **1**·THF inclusion compound **1a**. Displacement ellipsoids are drawn at the 30% probability level and numbering of relevant atoms is specified.



**Fig. 2** Packing diagram of **1**·THF (1 : 1), viewed down the *a*-axis. All hydrogen atoms are omitted for clarity.

conformation of **1** is asymmetric (Fig. 3). The host molecules possess a length of approximately 17.7 Å which is about 2 Å shorter compared to the above THF inclusion complex. This is due to a rather distinct bend along the tetraethynylene chain showing a deviation of 10.3° from linearity. Also this property can be ascribed to packing effects in the crystal. Nevertheless, the bond distances within the C<sub>8</sub>-fragment are nearly the same as for the THF inclusion case, showing that bending is a softer parameter of the spacer unit than stretching or shortening of bonds. With reference to the guest cyclohexanol molecules, three of them (guests 1, 2 and 4) are disordered over two positions, each having an occupancy factor of 0.5. The fourth cyclohexanol molecule (guest 3) is disordered around the symmetry center  $\frac{1}{2}, \frac{1}{2}, 0$ . In one of its orientations, hydrogen bonding between H(1K) and O(1N) of guest molecule 4 occurs, whereas in the inverse orientation the oxygen atom O(1K) is involved in hydrogen bonding with guest molecule 1 (Fig. 4a).

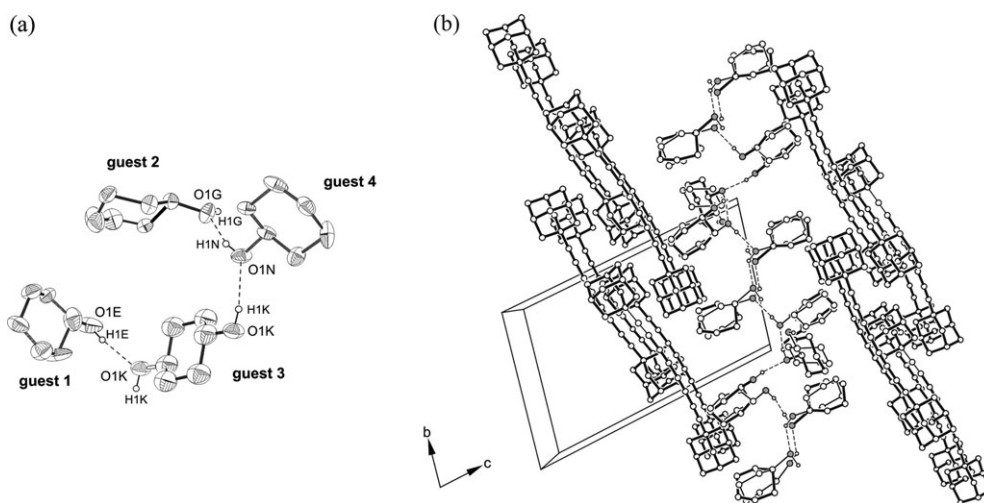
The packing structure as a whole is composed of alternating layers of host and guest molecules extending parallel to the crystallographic *ab*-plane (Fig. 4b). Within the host domains, all molecular rods are aligned along the *b*-axis. In order to realize close-packing, adjacent host molecules are displaced



**Fig. 3** Molecular structure of the **1**·cyclohexanol inclusion compound **1b**. Displacement ellipsoids are drawn at the 30% probability level and numbering of relevant atoms is specified.

along the rod direction such that their bulky adamantyl residues fit around the C<sub>8</sub>-unit. In this way, each C<sub>8</sub>-chain is surrounded by four adamantyl groups of four molecules. The molecular offset allows effective host–host interactions of the C–H···π type<sup>15,16</sup> with a closest contact distance of 2.76 Å. The most remarkable feature of the inclusion compound structure is that nearly one half of the crystal volume is occupied by cyclohexanol molecules. They are associated by a close network of hydrogen bonds in which all strong donors and acceptors take part (Table 2). The non-polar parts of the molecules are facing the hydrophobic surface of the host layers, so that the core region of the guest layers is defined by the polar O–H groups.

The inclusion compound between **1** and aniline (**1c**) crystallizes in the triclinic space group *P* $\bar{1}$ , with one and a half

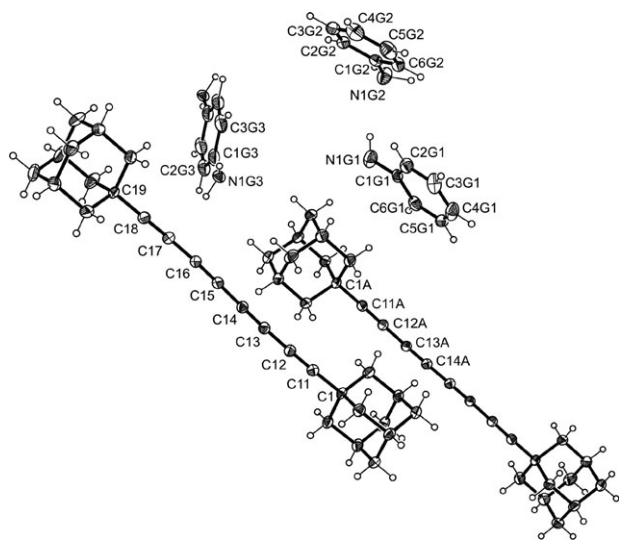


**Fig. 4** Packing of **1**·cyclohexanol (2 : 7). (a) Excerpt showing the cluster of H-bonded cyclohexanol molecules. Only one of the disordered positions of cyclohexanol molecules 1, 2 and 4 is illustrated. (b) Packing diagram viewed down the *a*-axis. Only the hydrogen atoms involved in intermolecular connections are depicted. Disordered positions of the cyclohexanol molecules are specified with thin and bold lines.

**Table 2** Distances (Å) and angles (°) of hydrogen bond interactions

	Atoms involved D—H...A	Symmetry	Distances		Angles D—H...A
			D...A	H...A	
<b>1</b> · Cyclohexanol (2 : 7)	Guest–guest				
	O(1E)–H(1E)...O(1K)	$-x, -y, 1 - z$	3.174(4)	2.46	146.3
	O(1G)–H(1G)...O(1M)	$x, y, z$	2.759(9)	1.95	168.7
	O(1H)–H(1H)...O(1E)	$1 + x, y, z$	2.738(4)	1.92	179.7
	O(1K)–H(1K)...O(1N)	$-x, -y, 1 - z$	2.780(4)	1.97	168.6
	O(1M)–H(1M)...O(1H)	$x, y, z$	2.740(4)	1.93	167.4
	O(1N)–H(1N)...O(1G)	$-x, -y, 2 - z$	2.745(3)	1.98	155.7
	Host–host				
	C(4)–H(4B)...C(13)	$-x, 1 - y, 1 - z$	3.668(6)	2.76	153.4
	C(8)–H(8)...C(17)	$1 - x, 1 - y, 1 - z$	5.579(6)	2.88	137.6
<b>1</b> · Aniline (3 : 5)	N(1G1)–H(2GA)...N(1G2)	$x, y, z$	3.256(4)	2.48	147.6
	N(1G1)–H(1GA)...C(13A)	$1 - x, -y, -z$	3.394(4)	2.51	147.0
	N(1G2)–H(1GB)...C(14A)	$1 + x, y, z$	3.497(3)	2.85	120.5
	N(1G2)–H(2GB)...centroid C	$1 + x, y, z$	3.401(4)	2.38	166.7
	N(1G3)–H(1GC)...centroid A	$-1 + x, y, z$	3.229(4)	2.36	154.7

independent host molecules and two and a half guest molecules in the asymmetric unit of the cell (Fig. 5). The reason for this unusual host–guest ratio can be seen as the presence of discrete pentameric units of guest molecules held together by two conventional N–H...N hydrogen bonds<sup>17</sup>  $> d(\text{N} \cdots \text{H})$  2.48 Å] and four N–H... $\pi$ (arene) contacts<sup>18,19</sup> (Fig. 6a). The central aniline molecule of the pentamer is disordered around the center of symmetry ( $0, \frac{1}{2}, 0$ ), and thus includes two positions for the coordinating amino group. The remaining amino hydrogens are associated with the host molecules *via* weak N–H... $\pi$ (alkyne) interactions.<sup>18,19</sup> Compared to the structure of the above cyclohexanol inclusion compound, here the C<sub>8</sub>-fragment of the host molecules is distorted to a lesser extent. The host molecule occupying the inversion center  $\frac{1}{2}, \frac{1}{2}, 0$  shows a slight S-shaped geometry, whereas the second host molecule is nearly linear. Their molecular lengths are 19.6 and 19.8 Å, respectively.

**Fig. 5** Molecular structure of the **1** · aniline inclusion compound **1c**. Displacement ellipsoids are drawn at the 50% probability level and numbering of relevant atoms is specified.

Another difference between the present structure (**1c**) and the previous structure (**1b**) is the packing, which is of a channel-type as contrasted with the layer formation of the cyclohexanol inclusion compound, thus being closer to the THF inclusion (Fig. 6b). In more detail, the structure of the aniline inclusion compound features elongated inclusion channels with a cross-section of approximately  $14.4 \times 9.5$  Å containing characteristic narrowings caused by the bulky adamantyl moieties that reduce the channel diameter to 9.1 Å. These channels contain the clustered aniline molecules.

### Unsolvated compounds 3–5

While compound **1** yielded crystalline inclusion compounds with a variety of different solvents (Table 1), respective crystallization of **2–5** produced only the unsolvated species, suggesting that these molecules due to their geometry and molecular dimensions permit close packing of themselves without the assistance of a guest solvent.<sup>20,21</sup> This may be seen from the crystal structures determined for **3–5**.

The structures of **3** and **4** are triclinic ( $P\bar{1}$ ,  $Z = 1$ ) and show some common features. Their ethynylene units deviate significantly from linearity to give the molecules with an S-shaped conformation (Fig. 7). The deviation of these units from linearity is  $10.4^\circ$  for compound **3** and  $6.7^\circ$  for **4**. The molecular lengths are 23.6 and 19.0 Å, respectively.

Although compound **3** is potentially capable of forming  $\pi$ – $\pi$ -contacts, neither aromatic nor ethynylene groups participate in this kind of interaction. Instead, a parallel alignment of molecular rods is observed in the crystalline packing with the molecules being subjected to weak hydrophobic interactions (Fig. 8). Thus, the crystal structure of **3** consists of linear arrays of molecules packed by van der Waals forces. The longitudinal displacement between molecular strands, which was calculated from the distance between the biphenyl center and the terminal hydrogen of the adamantyl unit, is approximately 11.8 Å. This arrangement enables interactions between adamantyl groups and aromatic units with a closest C–H...C contact distance of 2.8 Å.



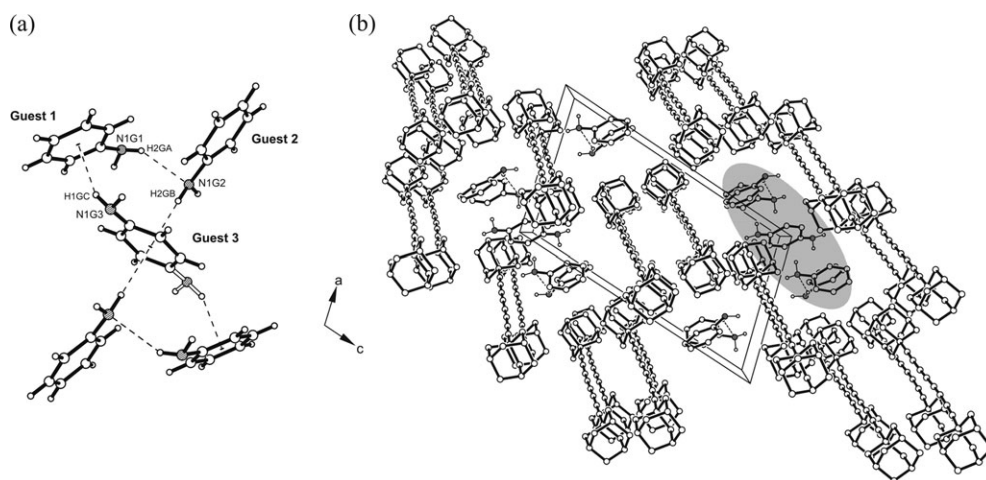


**Fig. 6** Packing of **1** · aniline (3 : 5). (a) Excerpt showing the cluster of H-bonded aniline molecules. (b) Packing diagram viewed down the *b*-axis. Only the hydrogen atoms involved in intermolecular connections are depicted. The shaded area represents the H-bonded aniline cluster.

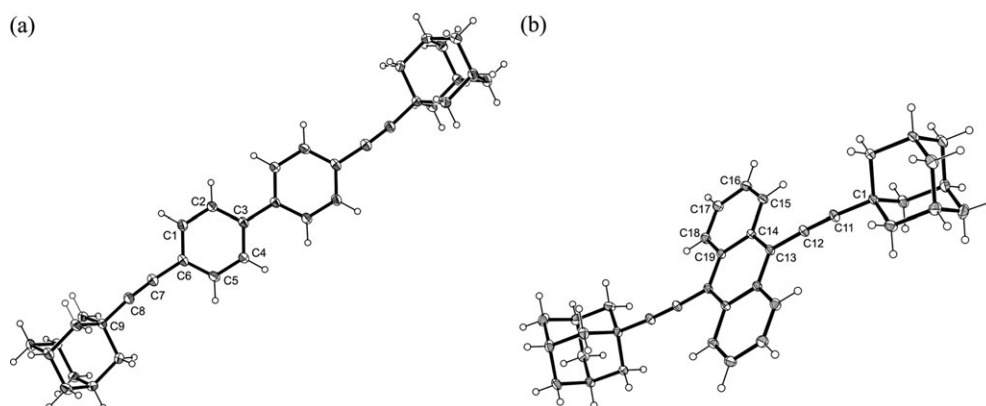


**Fig. 7** Molecular structure of (a) **3** and (b) **4**. Displacement ellipsoids are drawn at the 50% probability level and numbering of relevant atoms is specified.

The molecular arrangement in the crystal structure of the anthracene derivative **4** is similar to **3** though the pattern of molecular interactions is rather different, which can be attributed to a shorter molecular length and the presence of a more extended aromatic building block in compound **4** (Fig. 9). The longitudinal offset between adjacent molecules, which is nearly half the molecular length (8.5 Å), shifts the adamantyl moieties

into the voids of neighboring molecules left by their short acetylene fragments. There is also a significant overlap between the outer rings of the anthracene units so that aromatic stacking interactions stabilize the crystal structure along the crystallographic *b*-axis.<sup>22</sup>

Although having inherent  $C_3$  symmetry, compound **5** crystallizes in the monoclinic space group *Cc*. The asymmetric unit of the cell contains two crystallographically independent

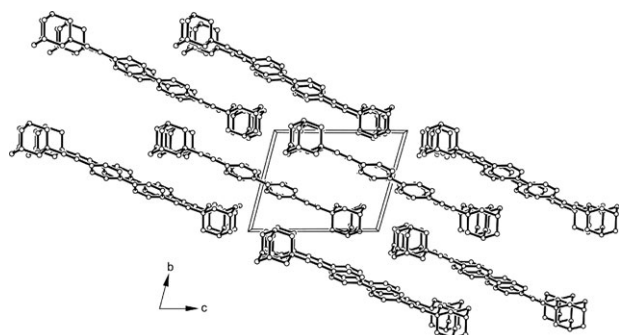


**Fig. 8** Packing diagram of **3**, viewed down the *a*-axis. All hydrogen atoms are omitted for clarity.

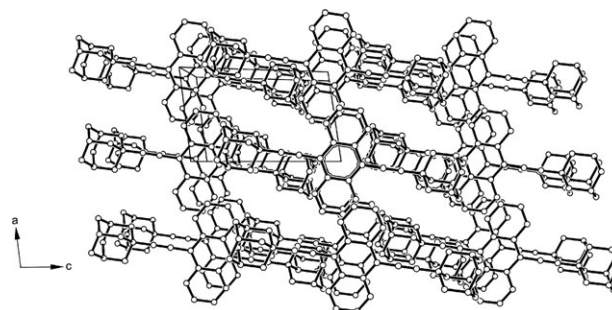


**Fig. 9** Packing diagram of **4**, viewed down the *b*-axis. All hydrogen atoms are omitted for clarity.

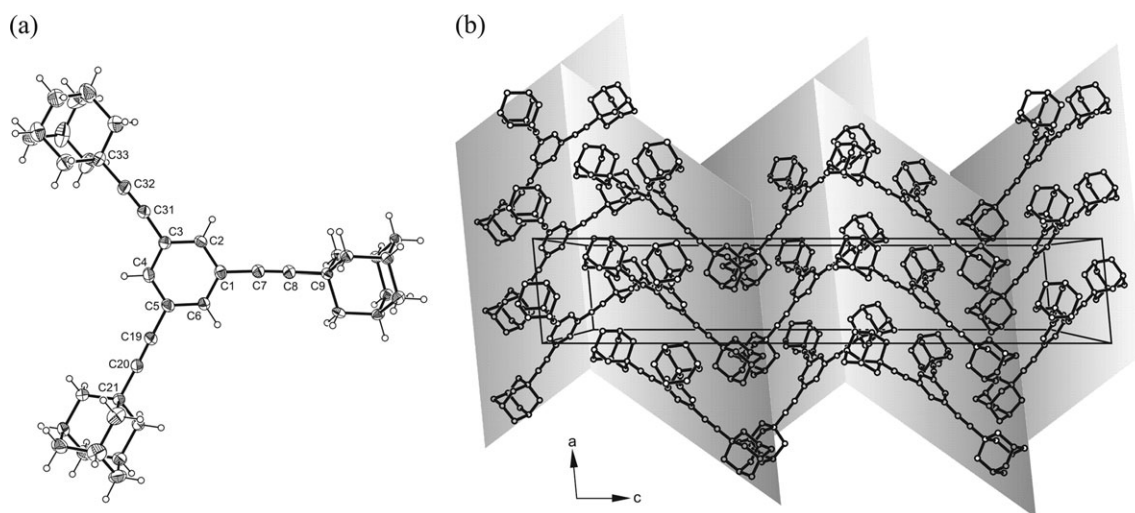


**Fig. 10** (a) Molecular structure of **5**. Displacement ellipsoids are drawn at the 50% probability level and numbering of relevant atoms is specified. (b) Packing diagram of **5**, viewed down the *b*-axis. All hydrogen atoms are omitted for clarity. The folded sheet structure is illustrated by shading.

molecules being nearly perpendicular to each other. As they show nearly identical conformations, only one of them is illustrated in Fig. 10a. The crystal packing of **5** is characterized by a columnar arrangement of molecules with an intermolecular distance equal to the length of the crystallographic *a*-axis (Fig. 10b). In a similar manner to the rod-like analogues **3** and **4**, the packing structure of **5** is controlled by geometric rather than electronic factors.

## Conclusions

The structural principles to efficiently yield a crystalline inclusion host (clathrate host) have been elaborated in different ways, including bulkiness, rigidity and functional groups as the main molecular parameters.<sup>10,23</sup> Moreover, concepts of crystal engineering<sup>8,24</sup> and the supramolecular synthon approach<sup>25</sup> add to this, giving rise to basic structures such as the scissor-type, roof-shaped, wheel-and-axle or dumb-bell shaped host molecules.<sup>6,7</sup> Although molecules having distinctive character of these classes of compounds are prone to form a crystalline host, rather small structural modifications may improve or impair its inclusion property. This has been studied in this paper by a series of compounds **1–5** having gradually modified structures, which lead to the following statements and conclusions.

The dumb-bell shaped prototype compound **1** exhibits versatility of crystalline inclusion behavior as illustrated in Table 1 and consolidated by the crystal structures. Here, channel or layer structures are typical of the built-up host lattice, dependent on the size and nature of the included guest solvent, thus showing structural variability. According to the hydrophobic nature of the host molecule, interactions between host and guest components are not significant while protic solvents are included as H-bonded clusters of guest molecules. On the other hand, the modified structures **2–4** turned out to be totally inefficient at forming inclusion complexes using corresponding recrystallization conditions. This indicates that

gradual substitution of ethynylene units of the central spacer axis of compound **1** by arylene groups, without alteration of the global linear structure of the molecule, prevents formation of crystalline inclusion compounds. Structural analyses have shown that C–H... $\pi$ <sup>15,16</sup> and  $\pi$ -stacking interactions,<sup>22</sup> aside from lateral spatial effects due to the aromatic groups, are responsible for a better fit and sticking together of the molecules in the respective crystal packings. Similarly this is true for the trigonal analogue of compound **2**, *i.e.* compound **5**, involving a more drastic operation on the molecular shape. However, previous linear analogues of the prototype molecule **1** having a shortened ethynylene spacer element, which may not be expected to produce such a strong effect, also leads to failure of crystalline inclusion compound formation.<sup>11</sup>

Thus, making structural changes on an exemplary clathrate host, however small they may be, may lead to drastic changes in its enclathrating abilities. This points to the delicate relations between molecular and packing parameters controlling the host behavior in the solid state. More detailed studies are required to go into the true facts behind this problem.

## Experimental

### Methods and materials

Melting points were determined on a Kofler melting point microscope (VEB Dresden Analytik) and were not corrected. NMR spectra were recorded on a Bruker Avance DPX 400 spectrometer with Me<sub>4</sub>Si (in CDCl<sub>3</sub>) as internal standard at 25 °C with 400 MHz for <sup>1</sup>H NMR and 100 MHz for <sup>13</sup>C NMR. Mass spectra were recorded on a Varian MAT 2/2 mass spectrometer. Elemental analyses were determined on a Heraeus CHN rapid analyzer.

All reactions were monitored by thin-layer chromatography (TLC) carried out on Merck silica gel 60 F<sub>254</sub> coated plates with UV light, iodine, concentrated sulfuric acid and heat as developing agents. Merck silica gel (60, particle size 0.063–

0.1 mm) was used for column chromatography. Organic solvents were purified by standard procedures.<sup>25</sup>

1,4-dibromobenzene, 4,4'-dibromobiphenyl, 9,10-dibromoanthracene and 1,3,5-tribromobenzene were purchased from commercial suppliers.

## Synthesis

1-Ethynyladamantane (**6**) was prepared according to the literature procedures.<sup>11,12</sup> Compound **1** was synthesized as described previously.<sup>11</sup>

**Compounds 2–5. General procedure.** A solution of the respective bromoarene (10 mmol) in diethylamine–toluene (1 : 1, 100 ml) was heated under reflux for 15 min while argon was passed through the solution to expel air. After addition stoichiometric amounts of the acetylenic compound **6** (22 or 33 mmol, respectively), the solution was cooled down to room temperature. The catalyst composed of palladium(II) acetate (25 mg), triphenylphosphane (75 mg), and copper(I) iodide (25 mg) was added and the mixture refluxed for 20 h. A precipitate of triethylamine hydrochloride which was formed on cooling down to room temperature was separated, added to 6 M hydrochloric acid and extracted with diethyl ether. The combined organic phases were washed with 1 M hydrochloric acid, saturated aqueous sodium hydrogen carbonate and sodium chloride, in this sequence, and dried (sodium sulfate). The solvent was evaporated and the crude product purified by column chromatography (silica gel, eluent: *n*-hexane). Further details and data of the individual compounds are given below.

**1,4-Bis[2-(1-adamantyl)ethynyl]benzene (2).** 1,4-Dibromobenzene (2.36 g, 10 mmol) was used; yield 71%; mp 231–234 °C. <sup>1</sup>H NMR (400 MHz, CDCl<sub>3</sub>): δ = 1.7 (m, 12 H, CHCH<sub>2</sub>C), 1.9 (m, 12 H, CHCH<sub>2</sub>CH), 2.0 (m, 6 H, CH<sub>2</sub>CHCH<sub>2</sub>), 7.3 (s, 4 H, ArH). <sup>13</sup>C NMR (100 MHz, CDCl<sub>3</sub>): δ = 28.1 (CH<sub>2</sub>CHCH<sub>2</sub>), 30.2 (C-quat.), 36.4 (CHCH<sub>2</sub>CH), 42.9 (CHCH<sub>2</sub>C), 79.4 (Ar–C≡C), 99.7 (Ar–C≡C), 123.3, 131.4 (C–Ar). MS (EI, 70 eV): *m/z* (%): 394 (M<sup>+</sup>, 100), 337 (42), 135 (15). Anal. calcd for C<sub>30</sub>H<sub>34</sub>: C, 91.32; H, 8.68; found: C, 91.34; H, 8.88.

**4,4'-Bis[2-(1-adamantyl)ethynyl]biphenyl (3).** 4,4'-Dibromobiphenyl (3.12 g, 10 mmol) was used; yield 76%; mp 322–326 °C. <sup>1</sup>H NMR (400 MHz, CDCl<sub>3</sub>): δ = 1.5 (m, 12 H, CHCH<sub>2</sub>C), 2.0 (m, 12 H, CHCH<sub>2</sub>CH), 2.1 (m, 6 H, CH<sub>2</sub>CHCH<sub>2</sub>), 7.4 (d, <sup>3</sup>J<sub>H, H</sub> = 8 Hz, 4 H, ArH), 7.5 (<sup>3</sup>J<sub>H, H</sub> = 8 Hz, 4 H, ArH). <sup>13</sup>C NMR (100 MHz, CDCl<sub>3</sub>): δ = 28.1 (CH<sub>2</sub>CHCH<sub>2</sub>), 30.2 (C-quat.), 36.5 (CHCH<sub>2</sub>CH), 43.0 (CHCH<sub>2</sub>C), 79.3 (Ar–C≡C), 99.3 (Ar–C≡C), 123.4 (C–Ar–C≡C), 126.6, 132.7, 139.5 (C–Ar). MS (EI, 70 eV): *m/z* (%): 470 (M<sup>+</sup>, 100), 427 (3), 413 (20). Anal. calcd for C<sub>36</sub>H<sub>38</sub>: C, 91.86; H, 8.14; found: C, 91.93; H, 8.25.

**9,10-Bis[2-(1-adamantyl)ethynyl]anthracene (4).** 9,10-Dibromoanthracene (3.36 g, 10 mmol) was used; 43%, mp 321–324 °C. <sup>1</sup>H NMR (400 MHz, CDCl<sub>3</sub>): δ = 1.8 (m, 12 H, CHCH<sub>2</sub>C), 2.1 (m, 6 H, CH<sub>2</sub>CHCH<sub>2</sub>), 2.2 (m, 12 H, CHCH<sub>2</sub>CH), 7.6 (q, <sup>3</sup>J<sub>H, H</sub> = 3.2 Hz, 4 H, Ar–H), 8.5 (q, <sup>3</sup>J<sub>H, H</sub> = 3.2 Hz, 4 H, Ar–H). <sup>13</sup>C NMR (100 MHz, CDCl<sub>3</sub>): δ = 28.2 (CH<sub>2</sub>CHCH<sub>2</sub>), 31.1 (C-quat.), 36.5 (CHCH<sub>2</sub>C), 43.2 (CHCH<sub>2</sub>C) 76.3 (Ar–C≡C), 111.3 (Ar–C≡C), 118.4, 126.2,

**Table 3** Crystallographic and structure refinement data of the compounds studied

Compound	<b>1a</b> <sup>a</sup>	<b>1b</b> <sup>b</sup>	<b>1c</b> <sup>c</sup>	<b>3</b>	<b>4</b>	<b>5</b>
Empirical formula	2(C <sub>28</sub> H <sub>30</sub> ) · 2 (C <sub>4</sub> H <sub>8</sub> O)	C <sub>28</sub> H <sub>30</sub> · 3.5(C <sub>6</sub> H <sub>12</sub> O)	1.5(C <sub>28</sub> H <sub>30</sub> ) · 2.5(C <sub>6</sub> H <sub>7</sub> N)	C <sub>36</sub> H <sub>38</sub>	C <sub>38</sub> H <sub>38</sub>	C <sub>42</sub> H <sub>48</sub>
Formula weight	877.31	436.60	782.60	470.66	494.68	552.80
Crystal system	Monoclinic	Triclinic	Triclinic	Triclinic	Triclinic	Monoclinic
Space group	<i>P</i> 2 <sub>1</sub> / <i>c</i>	<i>P</i> 1	<i>P</i> 1	<i>P</i> 1	<i>P</i> 1	<i>C</i> <i>c</i>
<i>a</i> /Å	21.7567(7)	10.540(1)	10.7534(6)	6.401(3)	6.6620(2)	6.853(3)
<i>b</i> /Å	12.5555(4)	11.616(1)	11.5581(6)	9.533(3)	10.1600(3)	25.898(3)
<i>c</i> /Å	19.2403(6)	18.944(6)	19.0689(11)	11.538(3)	11.1284(3)	37.211(3)
<i>α</i> /°	90.0	101.42(1)	98.037(3)	103.85(3)	114.744(2)	90.0
<i>β</i> /°	109.834(2)	104.02(1)	105.183(3)	92.84(3)	92.734(2)	95.29(3)
<i>γ</i> /°	90.0	98.35(1)	99.764(3)	105.71(3)	101.360(2)	90.0
<i>V</i> /Å <sup>3</sup>	4944.0(3)	2159.7(7)	2211.5(2)	653.1(1)	663.47(3)	6576.1(30)
<i>Z</i>	4	2	2	1	1	8
<i>F</i> (000)	2044	788	788	254	266	2400
<i>ρ</i> <sub>c</sub> /g cm <sup>−3</sup>	1.179	1.103	1.175	1.258	1.238	1.117
<i>μ</i> /mm <sup>−1</sup>	0.074	0.511	0.067	0.499	0.069	0.463
Temperature (K)	93(2)	178(2)	93(2)	133(2)	93(2)	183(2)
Measured reflections	86450	9117	52178	2918	49528	7361
Within the <i>θ</i> -limit (°)	0.99–29.0	2.5–74.6	1.1–28.2	4.0–74.7	2.3–45.7	2.4–74.9
Index ranges <i>±h</i> , <i>±k</i> , <i>±l</i>	−29/29, −16/17, −26/26	−13/12, −14/14, 0/23	−14/14, −15/15, −25/25	0/8, −11/11, −14/14	−13/13, −20/20, −22/22	0/8, 0/32, −46/46
No. of unique reflections	13155	8839	10895	2667	11373	7360
<i>R</i> <sub>int</sub>	0.0696	0.0213	0.0470	0.0129	0.0288	0.1086
No. of refined parameters	604	778	656	240	172	757
No. of <i>F</i> <sup>2</sup> values used [ <i>I</i> > 2σ( <i>I</i> )]	8801	7135	7383	2219	8033	5907
<i>R</i> <sub>1</sub> [ <i>I</i> > 2σ( <i>I</i> )]	0.0613	0.0993	0.0470	0.0385	0.0448	0.0696
w <i>R</i> <sub>2</sub> [ <i>I</i> > 2σ( <i>I</i> )]	0.1422	0.2639	0.0678	0.1050	0.1158	0.1852

<sup>a</sup> **1** · THF (1 : 1). <sup>b</sup> **1** · cyclohexanol (2 : 7). <sup>c</sup> **1** · aniline (3 : 5).



127.3, 132.0 (C–Ar). MS (EI, 70 eV):  $m/z$  (%): 494 ( $M^+$ , 100), 291 (6), 135 (6). Anal. calcd for  $C_{38}H_{38}$ : C, 92.25; H, 7.75; found: C, 92.10; H, 7.93.

**1,3,5-Tris[2-(1-adamantyl)ethynylbenzene] (5).** 1,3,5-Tribromobenzene (3.15 g, 10 mmol) was used; 27%, mp 263–264 °C.  $^1H$  NMR (400 MHz,  $CDCl_3$ )  $\delta$  = 1.7 (m, 18 H,  $CHCH_2C$ ), 1.9 (m, 18 H,  $CHCH_2CH$ ), 2.0 (m, 9 H,  $CH_2CHCH_2$ ), 7.3 (s, 3 H, ArH).  $^{13}C$  NMR (100 MHz,  $CDCl_3$ ):  $\delta$  = 28.4 ( $CH_2CHCH_2$ ), 30.4 (C–quat.), 36.8 ( $CHCH_2CH$ ), 43.2 ( $CHCH_2C$ ), 78.7 (Ar–C $\equiv$ C), 99.3 (Ar–C $\equiv$ C), 124.6, 133.9 (C–Ar). MS (EI, 70 eV):  $m/z$  (%): 552 ( $M^+$ , 100), 495 (8), 235 (8), 135 (17). Anal. calcd for  $C_{42}H_{48}$ : C, 91.30; H, 8.70; found C, 91.32; H, 8.84.

### Crystalline inclusion compounds

The host compound was dissolved with heating in a minimum amount of the respective guest solvent. After this had stood for 12 h at room temperature, the crystals that had formed were collected, washed with diethyl ether, and dried (1 h, 15 Torr, room temp.). Host : guest stoichiometric ratios were determined by  $^1H$  NMR integration. Data for each compound are given in Table 1.

### X-Ray structure determination

Single crystals of **1a–c** were grown by controlled evaporation from a solution of **1** in the respective solvents. Crystals of **3**, **4** and **5** were obtained by crystallization from 2-butanone.

Data collections on **1a**, **1c** and **4** were performed on a Bruker APEX II CCD diffractometer ( $\lambda_{MoK\alpha}$  = 0.710 73 Å, graphite monochromator) by  $\varphi$ - and  $\omega$ -scans. The measured intensities were reduced to  $F^2$  and corrected for absorption with SADABS (SAINT-NT<sup>26</sup>). Structure solution, refinement and data output were carried out with the SHELXTL program package.<sup>27</sup> Refinement of coordination and anisotropic thermal parameters of non-hydrogen atoms was carried out by full-matrix least-squares refinement. All hydrogen atoms except those of the coordinating guest hydrogens in **1c** were generated geometrically and allowed to ride on their parent atoms. The amino hydrogens in structure **1c** were located experimentally from the electron density difference map. The X-ray diffraction data of **1b**, **3** and **5** were collected on a CAD4 diffractometer in the  $\omega$ – $2\theta$  scan mode ( $\lambda_{CuK\alpha}$  = 1.5418 Å, graphite monochromator). The SHELXS-97<sup>28</sup> program was applied for structure solution, while SHELXL-97<sup>29</sup> was used for structure refinement. All data were corrected for Lorentz and polarization effects. The corresponding crystallographic data are summarized in Table 3.†

### Acknowledgements

This work is part of the Graduate School Program (GRK 208) of the TU Bergakademie Freiberg supported by the Deutsche Forschungsgemeinschaft. T. M. is grateful for a scholarship from this organisation. E. W. also thanks the Fonds der

Chemischen Industrie for financial support. Part of this work has received support from the Swiss National Science Foundation.

### References

- 1 S. Höger, *Chem. Eur. J.*, 2004, **10**, 1320.
- 2 (a) A. C. Grimsdale and K. Müllen, *Angew. Chem.*, 2005, **117**, 5732 (*Angew. Chem., Int. Ed.*, 2005, **44**, 5592).
- 3 *Container Molecules and Their Guests, Monographs in Supramolecular Chemistry*, ed. D. J. Cram and J. M. Cram, Royal Society of Chemistry, Cambridge, UK, 1994, vol. 4.
- 4 T. Hertzsch, J. Hulliger, E. Weber and P. Sozzani, in *Encyclopedia of Supramolecular Chemistry*, ed. J. L. Atwood and J. W. Steed, Marcel Dekker, New York, 2004, p. 996.
- 5 V. Balzani, M. Venturi and A. Credi, *Molecular Devices and Machines*, Wiley-VCH, Weinheim, 2003.
- 6 *Inclusion Compounds*, ed. J. L. Atwood, J. E. D. Davies and D. D. MacNicol, Oxford University Press, Oxford, 1991, vol. 4.
- 7 *Comprehensive Supramolecular Chemistry*, ed. D. D. MacNicol, F. Toda and R. Bishop, Elsevier, Oxford, 1996, vol. 6.
- 8 *Design of Organic Solids, Topics in Current Chemistry*, ed. E. Weber, Springer-Verlag, Berlin-Heidelberg, 1998, vol. 198.
- 9 G. R. Desiraju, in *Crystal Design, Perspectives in Supramolecular Chemistry*, ed. G. R. Desiraju, Wiley, Chichester, 2003, vol. 7.
- 10 *Molecular Inclusion and Molecular Recognition – Clathrates II, Topics in Current Chemistry*, ed. E. Weber, Springer-Verlag, Berlin-Heidelberg, 1988, vol. 149.
- 11 T. Müller, J. Hulliger, W. Seichter, E. Weber, T. Weber and M. Wübbenhorst, *Chem. Eur. J.*, 2000, **6**, 54.
- 12 S. Takahashi, Y. Kuroyama, K. Sonogashira and N. Hagihara, *Synthesis*, 1980, 627.
- 13 H. Stetter and P. Goebel, *Chem. Ber.*, 1962, **95**, 1039.
- 14 Q. B. Boxterman, H. Hogeveen and R. F. Kingma, *Tetrahedron Lett.*, 1986, **27**, 1055.
- 15 M. Nishio, M. Hirota and Y. Umezawa, *The CH/ $\pi$  Interaction, Evidence, Nature, and Consequences*, Wiley-VCH, New York, 1998.
- 16 M. Nishio, *CrystEngComm*, 2004, **6**, 130.
- 17 G. A. Jeffrey, *An Introduction to Hydrogen Bonding*, Oxford University Press, Oxford, 1997.
- 18 G. R. Desiraju and T. Steiner, *The Weak Hydrogen Bond in Chemistry and Structural Biology*, Oxford University Press, Oxford, 1999.
- 19 M. Nishio, in *Encyclopedia of Supramolecular Chemistry*, ed. J. L. Atwood and J. W. Steed, Marcel Dekker, New York, 2004, p. 1576.
- 20 A. I. Kitaigorodskii, *Molecular Crystals and Molecules*, Academic Press, New York, 1973.
- 21 A. I. Kitaigorodskii, *Mixed Crystals, Solid State Sciences*, Springer-Verlag, Berlin-Heidelberg, 1984, vol. 33.
- 22 (a) E. A. Meyer, R. K. Castellano and F. Diederich, *Angew. Chem.*, 2003, **115**, 1244 (*Angew. Chem., Int. Ed.*, 2003, **42**, 1210).
- 23 E. Weber, in *Comprehensive Supramolecular Chemistry*, ed. D. D. MacNicol, F. Toda and R. Bishop, Elsevier, Oxford, 1996, vol. 6, p. 535.
- 24 *The Crystal as a Supramolecular Entity, Perspectives in Supramolecular Chemistry*, ed. G. R. Desiraju, Wiley, Chichester, 1996.
- 25 (a) G. R. Desiraju, *Angew. Chem.*, 1995, **107**, 2541 (*Angew. Chem., Int. Ed. Engl.*, 1995, **34**, 2311).
- 26 *SAINT-NT Version 6.0*, Bruker Analytical X-ray Systems, Madison, WI, USA, 2003.
- 27 *SHELXTL-NT Version 6.10*, Bruker Analytical X-ray Systems, Madison, WI, USA, 2000.
- 28 G. M. Sheldrick, *SHELXS-97, Program for solution of crystal structures*, University of Göttingen, Germany, 1997.
- 29 G. M. Sheldrick, *SHELXL-97, Program for refinement of crystal structures*, University of Göttingen, Germany, 1997.

† CCDC reference numbers 119507 (**1b**), 288444 (**3**), 288445 (**4**), 288446 (**5**), 288447 (**1a**), and 288448 (**1c**). For crystallographic data in CIF or other electronic format see DOI: 10.1039/b516244k